REFERENCES

[1] S. B. Cohn, "Microwave bandpass filters containing high-Q dielectric resonator," *IEEE Trans. Microwave Theory Tech.*, vol. MTT-16, pp. 218–227, Apr. 1968.

[2] P. Guillon and Y. Garault, "Accurate resonant frequencies of dielectric resonators," *IEEE Trans. Microwave Theory Tech.*, vol. MTT-25, pp. 916–922, Nov. 1977.

[3] T. Itoh and R. S. Rudokas, "New methods for computing the resonant frequencies of dielectric resonators," *IEEE Trans. Microwave Theory Tech.*, vol. MTT-25, pp. 52–54 Jan. 1977.

[4] M. Jaworski and M. W. Pospieszalski, "An accurate solution of the cylinder dielectric resonator problem," *IEEE Trans. Microwave Theory Tech.*, vol. MTT-27, pp. 639–643, July 1979.

[5] A. Glisson, D. Kajfez, and J. James, "Evaluation of modes in dielectric resonators using a surface integral equation formulation," *IEEE Trans. Microwave Theory Tech.*, vol. MTT-31, pp. 1023–1029, Dec. 1983.

[6] K. A. Zaki and C. Chen, "New results in dielectric-loaded resonators," *IEEE Trans. Microwave Theory Tech.*, vol. MTT-34, pp. 815–824, July 1986.

[7] M. Yousefi, S. K. Chaudhuri, and S. Safavi-Naeini, "GIBC formulation for the resonant frequencies and field distribution of substrate-mounted dielectric resonator," *IEEE Trans. Antennas Propagat.*, vol. 42, pp. 38–46, Jan. 1994.

[8] Y. Chen *et al.*, "Tuning effects of cylindrical dielectric-loaded resonators," *Microwave Opt. Technol. Lett.*, vol. 15, no. 3, pp, 127–134, June 1997.

[9] J.-M. Guan and C.-C. Su, "Resonant frequencies and field distributions for shielded uniaxially anisotropic dielectric rod resonator by the FD-SIC method," *IEEE Trans. Microwave Theory Tech.*, vol. 45, pp. 1767–1777, Oct. 1997.

[10] R. E. Collin, *Foundations for Microwave Engineering*, 2nd ed. New York: McGraw-Hill, 1992, sec. 6.7.

[11] S. N. Karp and F. C. Karal, Jr., "Electromagnetic wave theory: Part I," in *Generalized Impedance Boundary Conditions with Application to Surface Wave Structures*, J. Brown, Ed. New York: Pergamon, 1967.

[12] H. Peng, "Study of whispering gallery models in double disk sapphire resonators," *IEEE Trans. Microwave Theory Tech.*, vol. 44, pp. 848–853, June 1996.

[13] J. Krupka, P. Blondy, D. Cros, P. Guillon, and R. G. Geyer, "Whispering gallery modes and permeability tensor measurements in magnetized ferrite resonators," *IEEE Trans. Microwave Theory Tech.*, vol. 44, pp. 1097–1102, July 1996.

[14] W. H. Von Aulock and C. E. Fay, *Linear Ferrite Devices for Microwave Applications*. New York: Academic, 1968, pp. 30–35.

Analysis of Propagation Characteristics and Field Images for Printed Transmission Lines on Anisotropic Substrates Using a 2-D-FDTD Method

Ming-sze Tong and Yinchao Chen

***Abstract*— In this paper, we apply an efficient two-dimensional (2-D) finite-difference time-domain (FDTD) algorithm onto an analysis of uniform transmission lines printed on various anisotropic substrates. By investigating the transverse resonant properties of the structures, we obtain their propagation characteristics, as well as the field images at specified frequencies. To eliminate the Gibbs phenomenon generated by a sudden time-stepping termination, we employ the Blackman–Harris window (BHW) function to truncate and modulate the entire time-domain fields, which leads to a significant time saving by comparing the conventional time-stepping termination.**

I. INTRODUCTION

The finite-difference time-domain (FDTD) method is a very powerful technique in solving the Maxwell's equations related to boundary-value problems, especially the transmission-line problems, conventionally by using three-dimensional (3-D) techniques [1]–[3]. One commonly known disadvantage of the conventional FDTD is that it requires large amounts of computer central processing unit (CPU) time and memory space to discretize all fields and medium parameters in the entire 3-D computation domain, and to iterate the FDTD algorithm until the fields stabilize. Recently, Xiao and Vahldieck presented a two-dimensional (2-D) FDTD algorithm to analyze microstrip lines, and Hofschen and Wolff improved the algorithm by using a time-domain series technique [4], [5]. Similarly, Chen and Mittra introduced the concept of transverse resonance to the FDTD for transmission-line analysis, and presented a one-dimensional (1-D) FDTD algorithm for analyzing axisymmetric waveguides [6]. In principle, these FDTD techniques are more accurate than the 3-D FDTD scheme for analyzing transmission lines since they take an advantage of the analytical nature of solutions along the longitudinal direction.

In this paper, following a similar approach used in [4]–[6], we apply an efficient 2-D FDTD algorithm onto an analysis of various transmission lines printed on anisotropic substrates. By investigating the transverse resonant properties of the structures, we obtain their propagation characteristics, as well as the field images at specified frequencies. For efficiency and accuracy, we employ the Blackman–Harris window (BHW) function to truncate and modulate the entire time-domain fields rather than following the conventional rectangular windowing time-stepping termination, which leads to a significant time saving by reducing the total number of iterations.

II. FDTD ALGORITHM AND IMPLEMENTATION

To ensure that the Maxwell's equations to be discretized are in the form of the FDTD algorithm which contains only real variables, we represent the field quantities in the form

$$\begin{bmatrix} \vec{E}(\vec{r},\, t) \\ \vec{H}(\vec{r},\, t) \end{bmatrix} = \begin{Bmatrix} [jE_x(x,\, y,\, t),\, jE_y(x,\, y,\, t),\, E_z(x,\, y,\, t)] \\ [H_x(x,\, y,\, t),\, H_y(x,\, y,\, t),\, jH_z(x,\, y,\, t)] \end{Bmatrix} \cdot e^{-j\beta z}. \tag{1}$$

Manuscript received July 11, 1996; revised March 2, 1998. This work was supported by the Hong Kong Polytechnic University under Grant V312.

The authors are with the Department of Electronic Engineering, Hong Kong Polytechnic University, Hong Kong.

Publisher Item Identifier S 0018-9480(98)07233-0.

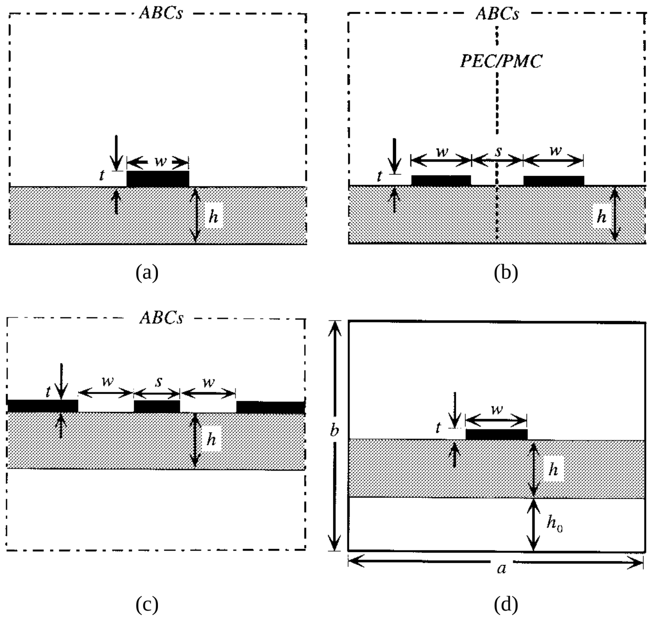

Fig. 1. Cross sections of the transmission lines. (a) Open single microstrip line. (b) Open coupled microstrip line. (c) Open unilateral CPW. (d) Shielded SML.

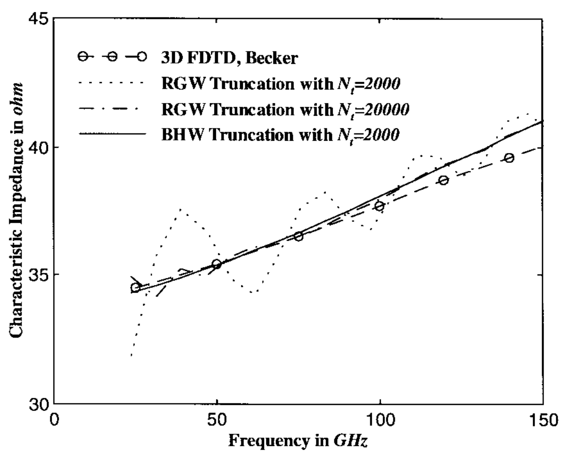

Fig. 2. Frequency dependence of Z_0 for an open single microstrip line with the RGW and BHW truncations ($N_x = 110$, $N_y = 30$, $\varepsilon_r = 13$, $\Delta x = \Delta y = 0.0125$, $h = 0.1$, $t = 0$, and $w = 0.15$ mm).

For generality, we assume that the relative permittivity, permeability, and electric conductivity are characterized as a diagonal tensor.

By substituting (1) into the Maxwell's equations, we obtain the compressed 2-D FDTD lattice and the expression of the 2-D update equations, typically, whose x-components are given by (2) and (3), shown at the bottom of the following page, where β is a specified propagation constant. The stability of the 2-D FDTD algorithm is ensured by choosing the time step Δt to satisfy the inequality suggested in [7]. Two types of absorbing boundary conditions (ABC's), the first-order Mur's and the dispersive ABC's [8], [9], are used to terminate meshes at the boundaries of open structures.

It is crucial in implementing the 2-D FDTD algorithm to accurately model the PEC strips and symmetric walls for analyzing printed transmission lines. Two types of strips, *viz*. the infinitesimally thin and the finite thickness, and two kinds of symmetric walls, i.e., perfectly electric conductor (PEC) and perfectly magnetic conductor (PMC), have been accurately modeled in this research. For modeling an

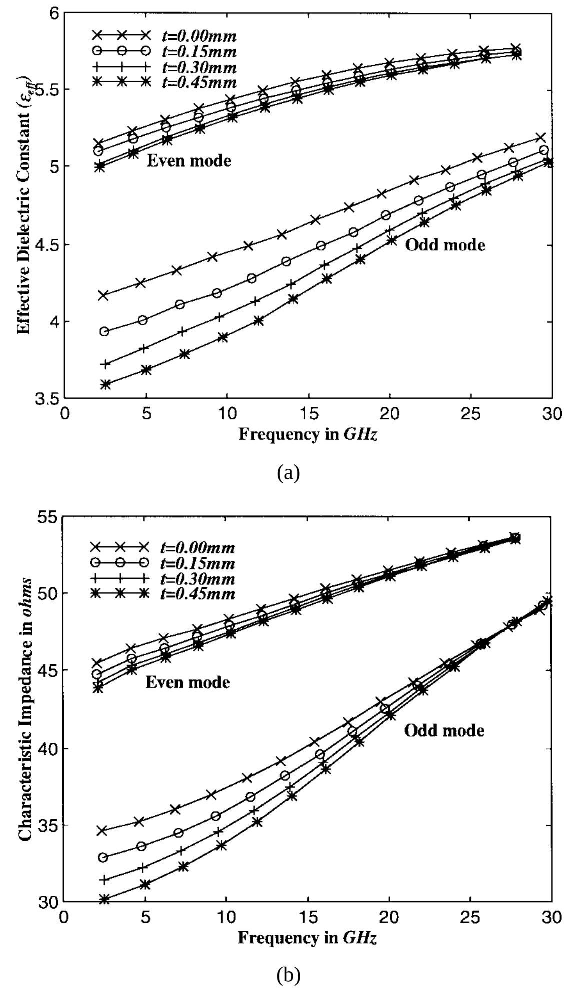

Fig. 3. Frequency dependence of propagation characteristics for an open coupled microstrip line printed on the filled PTFE (odd mode: $N_x = 39$, $N_y = 30, \Delta x = \Delta y = 0.15$; even mode: $N_x = 58.5, N_y = 30, \Delta x = 0.1$, $\Delta y = 0.15$; $h = s = 0.9$, $w = 1.8$ mm). (a) $\varepsilon_{\rm eff}$. (b) Magnitude of Z_0.

infinitesimally thin strip, we only let the components of conductivity $(\sigma_{xx},\, \sigma_{yy},\, \sigma_{zz})$ in a cell corresponding to the tangential E-fields to be infinite while keeping the rest at zero. Otherwise, for a finite-thickness strip, all components must be set to infinite. To model a PEC symmetric wall, we simply enforce the tangential electric fields to be zero along the wall. However, to model a PMC wall, rather than using image theory, in which the real and image fields are a half-cell away from the boundary [3], in a more accurate way, we set the tangential magnetic fields located at the centers of cells to zero.

Next, in order to eliminate the Gibbs phenomenon generated by a sudden truncation of time signals, which is equivalent to adding a rectangular window (RGW) function onto the time-domain signals, we use the BHW function [10] to modulate and truncate the field signals. Its extremely low sidelobe levels (less than -92 dB) and smooth main beam guarantee that the ripples of the window sidelobes will introduce little corruption into convoluted signals. The corresponding frequency-domain responses of the fields may be written as

$$[E_I^W(\omega),\, H_I^W(\omega)] = \int_0^\infty [E_I(\tau),\, H_I(\tau)] W_{BH}(\omega - \tau)d\tau, \qquad I = x,\, y,\, z \quad (4)$$

where ω is the radian frequency, $[E_I(\tau),\, H_I(\tau)]$ denote the original time-domain fields derived from the FDTD algorithm, and

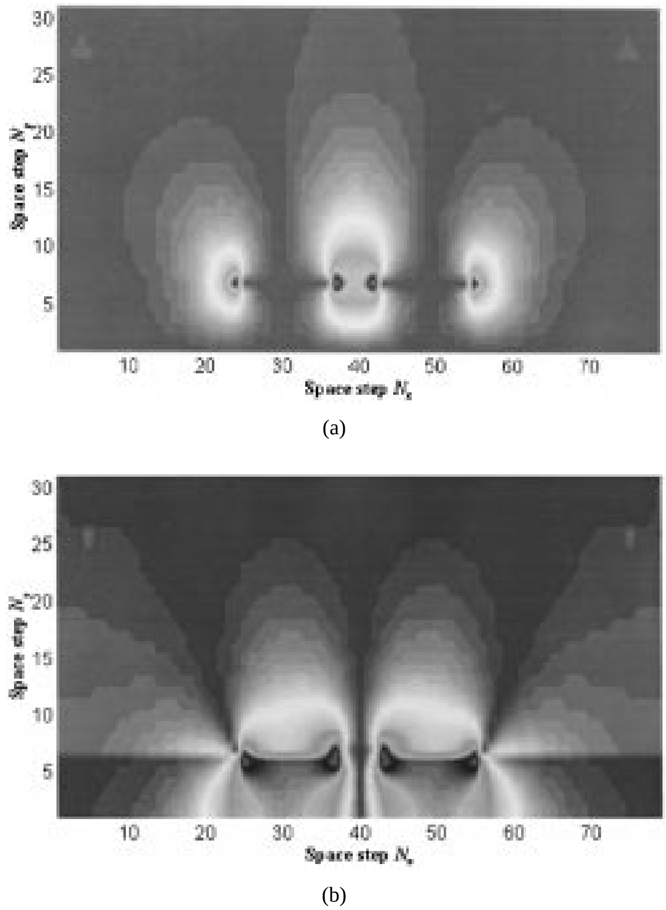

Fig. 4. Images of the normalized electric fields (odd mode) for an open coupled microstrip line with $t = 0$ at $\beta_0 = 500$ and $f_0 = 11.117$ GHz. (a) $\tilde{E}_x$. (b) $\tilde{E}_y$.

$[E_I^W(\omega), H_I^W(\omega)]$ are their windowed version in the frequency domain. Normally, the truncation with the RGW does not pose a problem for a time response that decays sufficiently and rapidly in time. However, such decay is relatively slow for resonant structures, and early truncation can lead to significant errors in results.

Finally, we have built the discrete Fourier transform (DFT) in our FDTD solver so that we can perform the DFT while updating the FDTD iterations. For a known resonant frequency f_0, the DFT is defined as

$$\tilde{E}_I(2\pi f_0, i, j) = \Delta t \sum_{n=0}^{N_t-1} E_I^n(i, j) \exp[-j2\pi f_0 n \Delta t], \quad I = x, y, z \tag{5}$$

where $i = 0, 1, 2, \ldots, N_x$, $j = 0, 1, 2, \ldots, N_y$, and E_I^n and $\tilde{E}_I$ denote the time-domain and frequency-domain fields, respectively.

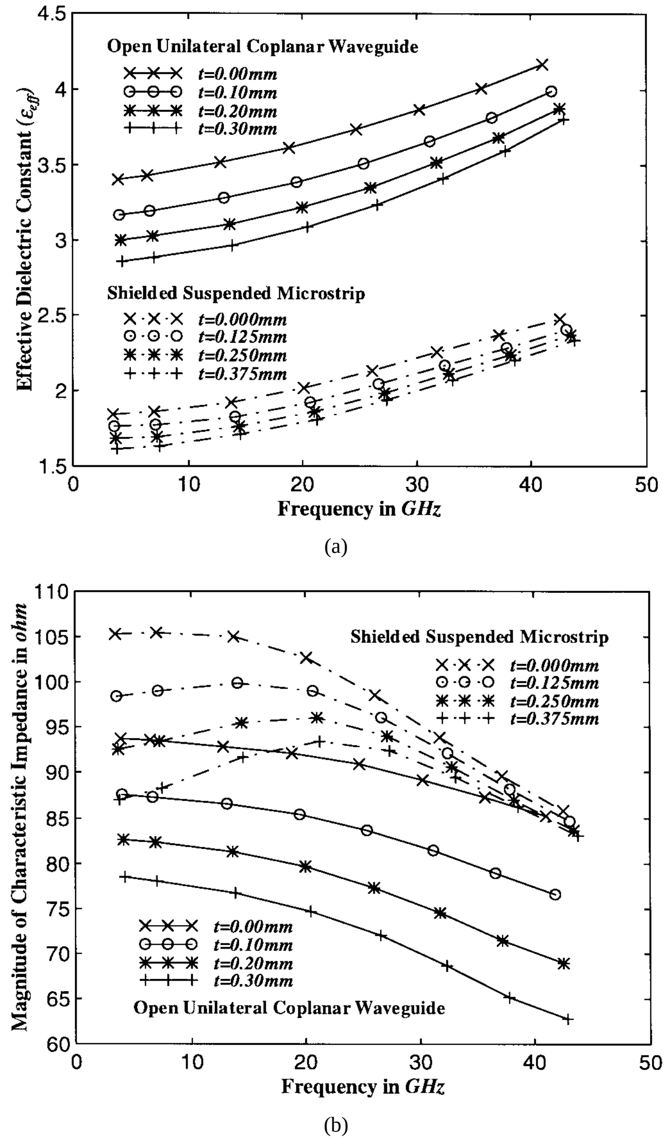

Fig. 5. Frequency dependence of propagation characteristics for an open unilateral CPW and a shielded SML (CPW: $N_x = 105$, $N_y = 60$, $\Delta x = \Delta y = 0.1$, $h = w = 1$, $s = 0.5$ mm; SML: $N_x = 56$, $N_y = 30$, $\Delta x = \Delta y = 0.125$, $a = 7$, $b = 3.75$, $w = h = h_0 = 0.75$ mm). (a) ε_{eff}. (b) Magnitude of Z_0.

III. Numerical Results

In this paper, we have analyzed various transmission lines, as shown in Fig. 1, printed on anisotropic substrates including the filled PTFE ($\varepsilon_{xx} = 6.64$, $\varepsilon_{yy} = 6.24$, $\varepsilon_{zz} = 5.56$) and boron nitride ($\varepsilon_{xx} = 5.12$, $\varepsilon_{yy} = 3.4$, $\varepsilon_{zz} = 5.12$).

Firstly, we would like to verify the effectiveness of the window modulation and truncation method by analyzing an open mi-

$$E_x^{n+1}(i+1/2, j) = \frac{1 - \frac{\Delta t \sigma_{xx}(i+1/2, j)}{[2\varepsilon_0 \varepsilon_{xx}(i+1/2, j)]}}{1 + \frac{\Delta t \sigma_{xx}(i+1/2, j)}{[2\varepsilon_0 \varepsilon_{xx}(i+1/2, j)]}} E_x^n(i+1/2, j) + \frac{\frac{\Delta t}{[\varepsilon_0 \varepsilon_{xx}(i+1/2, j)]}}{1 + \frac{\Delta t \sigma_{xx}(i+1/2, j)}{[2\varepsilon_0 \varepsilon_{xx}(i+1/2, j)]}} \cdot \left[\beta H_y^{n+1/2}(i+1/2, j) + \frac{H_z^{n+1/2}(i+1/2, j+1/2) - H_z^{n+1/2}(i+1/2, j-1/2)}{\Delta y}\right] \tag{2}$$

$$H_x^{n+1/2}(i, j+1/2) = H_x^{n-1/2}(i, j+1/2) + \frac{\Delta t}{\mu_0 \mu_{xx}(i, j+1/2)} \left[\beta E_y^n(i, j+1/2) - \frac{E_z^n(i, j+1) - E_z^n(i, j)}{\Delta y}\right] \tag{3}$$

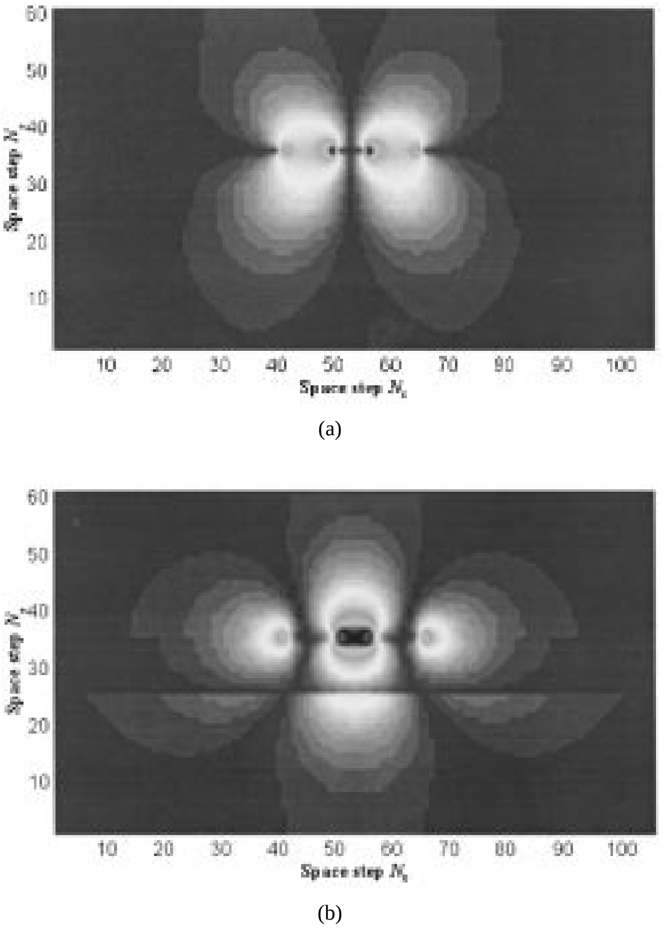

Fig. 6. Images of the normalized electric fields for an open unilateral CPW $(t = 0)$ at $\beta_0 = 500$ and $f_0 = 12.770$ GHz. (a) $\tilde{E}_x$. (b) $\tilde{E}_y$.

crostrip line, as defined in Fig. 1(a). The magnitude of characteristic impedance (Z_0) as a function of frequency for different numbers of iteration steps is shown in Fig. 2. As seen from this figure, the BHW modulation and truncation at $N_t = 2000$ leads to a smoother behavior of Z_0. Such results are even better than those generated by the RGW with $N_t = 20\,000$, in which the window size is ten times larger than the BHW one. With $N_t = 2000$, the RGW introduces unacceptably large errors. In this same figure, we also compare the computed results with those obtained by using the 3-D FDTD technique [3], and we observe a very good agreement within the frequency range of 25–75 GHz and a fairly good match from 75 to 150 GHz.

Next, we investigate an open coupled microstrip line, shown in Fig. 1(b), printed on the filled polytetrafluoroethylene (PTFE). As shown in Fig. 3, the propagation characteristics ε_{eff} and Z_0 of the odd mode are clearly much more sensitive to the variation of strip thickness than those of the even mode. We also display the normalized transverse-field distribution for the odd mode at a specified frequency in Fig. 4 for $t = 0$.

Finally, we analyze an open unilateral coplanar waveguide (CPW), see Fig. 1(c), and a shielded suspended microstrip line (SML, see Fig. 1(d), printed on the filled PTFE and on the boron nitrite, respectively. As the t varies, the corresponding ε_{eff} and Z_0 as functions of frequency displayed in Fig. 5 have changed significantly. It is found that the Z_0 of the SML is much sensible at the low frequencies, while its counterpart of the CPW varies uniformly. The electric field images of the CPW at a specified frequency with $t = 0$ are displayed in Fig. 6.

IV. Conclusion

An efficient 2-D FDTD algorithm has been applied for analyzing printed transmission lines on various isotropic and anisotropic substrates. The propagation characteristics has been studied by using the concept of the transverse resonant properties of the guided-wave structures, and the frequency-domain field images are obtained by using a DFT technique built in the FDTD solver.

References

[1] X. Zhang, J. Fang, K. K. Mei, and Y. Liu, "Calculations of the dispersive characteristics of microstrips by the time-domain finite difference method," *IEEE Trans. Microwave Theory Tech.*, vol. 36, pp. 263–267, Feb.1988.

[2] D. M. Sheen, S. M. Ali, M. D. Abouzahra, and J. A. Kong, "Application of the three-dimensional finite-difference time-domain method to the analysis of planar microstrip circuits," *IEEE Trans. Microwave Theory Tech.*, vol. 38, pp. 849–857, July 1990.

[3] W. D. Becker, "The Application of time-domain electromagnetic field solvers to computer package analysis and design." Ph.D. dissertation, Dept. Elect. Computer Eng., Univ. Illinois at Urbana-Champaign, 1993.

[4] S. Xiao and R. Vahldieck, "An efficient 2-D FDTD algorithm using real variables," *IEEE Microwave Guided Wave Lett.*, vol. 3, pp. 127–129, May 1993.

[5] S. Hofschen and I. Wolff, "Improvements of the two-dimensional FDTD method for simulation of normal- and superconducting planar waveguide using time series analysis," *IEEE Trans. Microwave Theory Tech.*, vol. 44, pp. 1487–1490, Aug. 1996.

[6] Y. Chen and R. Mittra, "A highly efficient finite difference time domain algorithm for analyzing axisymmetric waveguides," *Microwave Opt. Technol. Lett.*, vol. 15, no. 5, pp. 201–203, July 1997.

[7] A. C. Cangellaris, "Numerical stability and numerical dispersion of a compact 2-D/FDTD method used for the dispersion analysis of waveguides," *IEEE Microwave Guided Wave Lett.*, vol. 3, pp. 3–5, Jan. 1993.

[8] G. Mur, "Absorbing boundary conditions for finite difference approximation of the time domain electromagnetic-field equations," *IEEE Trans. Electromag. Compat.*, vol. EMC-23, pp. 1073–1077, Nov. 1981.

[9] Z. Bi, K. Wu, C. Wu, and J. Litva, "A dispersive boundary condition for microstrip component analysis using the FD-TD method," *IEEE Trans. Microwave Theory Tech.*, vol. 40, pp. 774–777, Apr. 1992.

[10] F. J. Harris, "On the use of windows for harmonic analysis with discrete Fourier transform," *Proc. IEEE*, vol. 66, pp. 51–83, Jan. 1978.